UP-TO-DATE RESULTS FROM THE PIERRE AUGER OBSERVATORY*

Bruno Zamorano

for the Pierre Auger Collaboration†

Departamento de Física Teórica y del Cosmos and CAFPE
Facultad de Ciencias, Universidad de Granada
Campus de FuenteNueva s/n, 18071 Granada, Spain

(Received October 21, 2013)

The Pierre Auger Observatory is a state-of-the-art cosmic ray detector, allowing one to analyse the properties of ultra-high energy cosmic rays with unprecedented precision. The observatory, covering an area of 3 000 km^2, combines two different detection techniques, making it the first of its kind. Here, we present some of the most relevant results obtained by this experiment.

DOI:10.5506/APhysPolB.44.2317
PACS numbers: 96.50.S–, 96.50.sb, 96.50.sd, 13.85.Tp

1. The Pierre Auger Observatory

The Pierre Auger Observatory [1] consists of the Surface Detector (SD), an array of 1660 water Cherenkov stations arranged on a triangular grid of 1500 m spacing for the main array and a 750 m spacing for a small infill area, and the Fluorescence Detector (FD), consisting of 27 air fluorescence telescopes that overlook the array.

The two detectors can work independently, making the Pierre Auger Observatory a hybrid detector. While the SD samples the particles arriving at the ground, providing information of the transversal footprint of the showers with nearly 100% duty cycle, the FD directly observes the longitudinal development of the showers with about 13% duty cycle, through the light produced by the de-excitation of nitrogen molecules. The advantages of having a hybrid detector include a better understanding of systematic uncertainties as well as a data-driven calibration of the detector.

* Presented at the XXXVII International Conference of Theoretical Physics "Matter to the Deepest" Ustroń, Poland, September 1–6, 2013.

† Observatorio Pierre Auger, Av. San Martín Norte 304, 5613 Malargüe, Argentina. Full author list: `http://www.auger.org/archive/authors_2013_06.html`

2. Measurement of the energy spectrum

The most distinct features of the flux above 10^{18} eV are a flattening of the spectrum at 4×10^{18} eV (the *ankle*) and a strong flux suppression above 5×10^{19} eV. A precise measurement of the flux at energies above 10^{17} eV is important for discriminating between different theoretical models [2, 3].

The amount of fluorescence light registered by the FD represents an almost model-independent calorimetric measurement of the energy deposited in the atmosphere by a shower. The energy measured by the FD, $E_{\rm FD}$, is obtained via the integration of the energy deposition as a function of atmospheric depth. Systematic uncertainty is about 14% [4].

The energy reconstruction of vertical events in the SD is based on the estimation of the number of secondary particles reaching ground at an optimal distance to the shower core. The signals $S(1000)$ and $S(450)$ (for the infill array) are corrected for their zenith angle dependence with a Constant Intensity Cut (CIC) method [5]. Inclined air-showers are characterised by the dominance of secondary muons at ground, so the reconstruction is based on the estimation of the relative muon content N_{19}. Events that independently trigger the SD and the FD, and pass strict quality cuts are used for the energy calibration of the SD.

The combined energy spectrum [6] is shown in Fig. 1. To characterise the spectral features, we describe the data with a broken power-law $J(E) \propto E^{-\gamma}$ with smooth suppression. γ_1, γ_2 are the spectral indices below/above the ankle at $E_{\rm a}$, $E_{1/2}$ is the energy at which the flux drops to a half, with steepness $\log_{10} W_c$. The resulting spectral parameters are given in Table I.

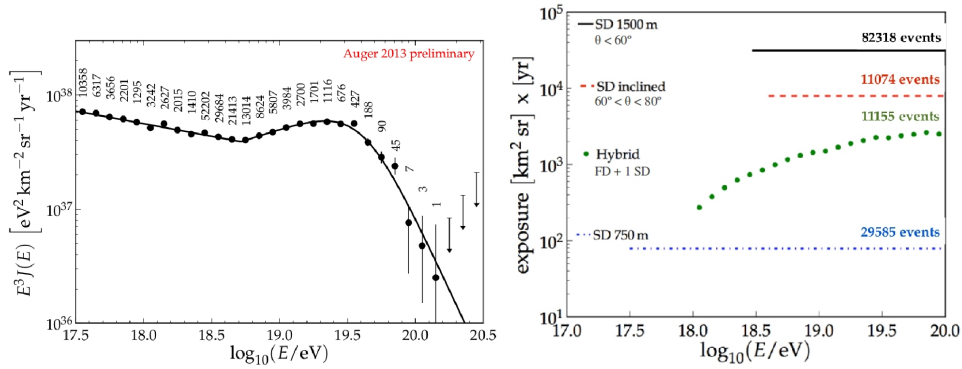

Fig. 1. The Pierre Auger Observatory combined spectrum (left). Relative exposure of the different datasets (right) [6].

TABLE I

Parameters of the parametrisation describing the combined energy spectrum measured at the Pierre Auger Observatory.

Parameter	Result $(\pm\sigma_{\rm stat} \pm \sigma_{\rm sys})$
$\log_{10}(E_{\rm a}/{\rm eV})$	$18.72 \pm 0.01 \pm 0.02$
γ_1	$3.23 \pm 0.01 \pm 0.07$
γ_2	$2.63 \pm 0.02 \pm 0.04$
$\log_{10}(E_{1/2}/{\rm eV})$	$19.63 \pm 0.01 \pm 0.01$
$\log_{10} W_c$	$0.15 \pm 0.01 \pm 0.02$

3. Mass composition

In order to unravel the astrophysical scenarios for cosmic ray production and propagation, the measurement of the energy spectrum needs to be complemented by an independent measurement of primary mass composition.

The FD can observe the longitudinal development of the electromagnetic component of the shower in a wide range of atmospheric depths. The position of the maximum of this profile $X_{\rm max}$ is used as a mass-sensitive parameter [5]. Not only the average value of $X_{\rm max}$ depends on the average mass of the primary cosmic rays, but also the spread of the distribution. Therefore, we can extract information related to mass-composition from $\langle X_{\rm max}\rangle$, and also from $\sigma\,(X_{\rm max})$. The results [7] obtained for these two parameters compared to different hadronic models are shown in Fig. 2.

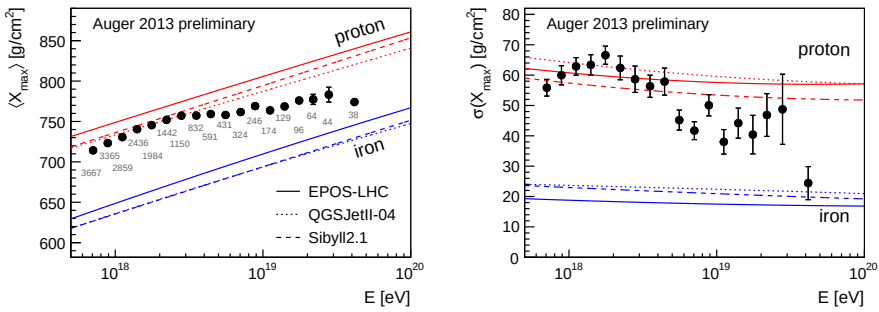

Fig. 2. Evolution of $\langle X_{\rm max}\rangle$ and $\sigma\,(X_{\rm max})$ with the energy [7].

The interpretation of these data [8] can be done advocating the superposition model (see *e.g.* [9]), which relates a certain measurement of $\langle X_{\rm max}\rangle$ $(\sigma^2\,(X_{\rm max}))$ with the predicted value of $\langle \ln A\rangle$ $(\sigma^2\,(\ln A))$, A being the mass number of the primary particle. The results are shown in Fig. 3. Within

uncertainties, the overall features are similar in all the cases. The data imply an increasing $\langle \ln A \rangle$ above $10^{18.3}$ eV from light to intermediate masses and a decreasing $\sigma^2(\ln A)$ over the whole energy range.

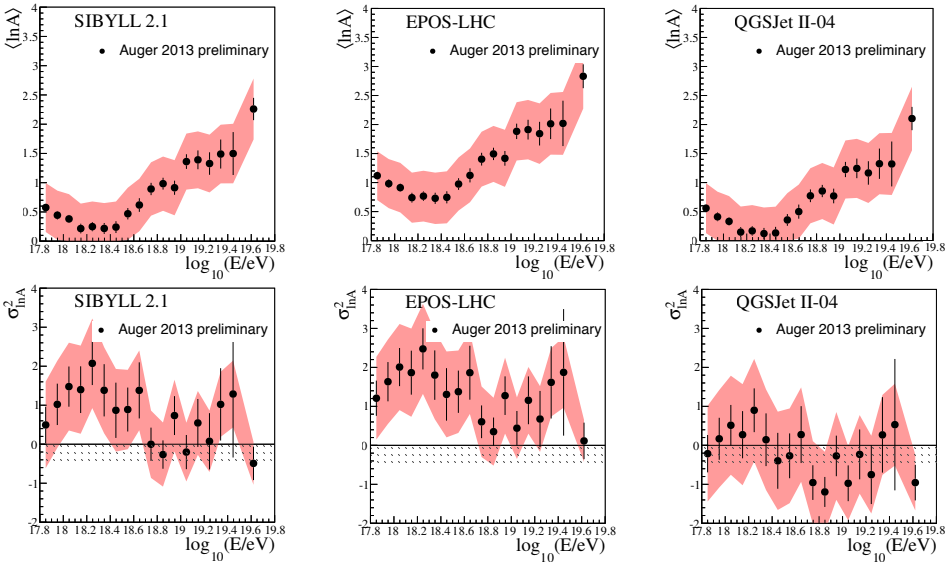

Fig. 3. Evolution of $\langle \ln A \rangle$ and $\sigma^2(\ln A)$ with $\log_{10} E$ [7].

4. Hadronic interactions

The interpretation of mass composition measurements is indiscernible from the description of high energy hadronic interactions. UHECRs (Ultra-high energy cosmic rays) can have energies up to one order of magnitude larger than the ones reached in the man-made experiments. It is useful then to extract hints about the hadronic interaction properties from UHECRs.

4.1. Cross-section

The tail of the $X_{\max}$ distribution is sensitive to the proton-air cross section. An exponential fit to the tail of this distribution provides

$$\frac{dN}{dX_{\max}} \propto \exp\left(\frac{-X_{\max}}{\Lambda_f}\right); \qquad \sigma_{p-\mathrm{air}} \propto \Lambda_f^{-1}. \tag{1}$$

Simulations are used to transform Λ_f into $\sigma_{p-\mathrm{air}}$ in the energy interval between 10^{18} and $10^{18.5}$ eV, the average energy corresponding to a center-of-mass energy in the nucleon–nucleon system of $\sqrt{s} = 57$ TeV. The final result is shown in Fig. 4

$$\sigma_{p-\mathrm{air}} = \left[505 \pm 22(\mathrm{stat})^{+28}_{-36}(\mathrm{sys})\right] \ \mathrm{mb}. \tag{2}$$

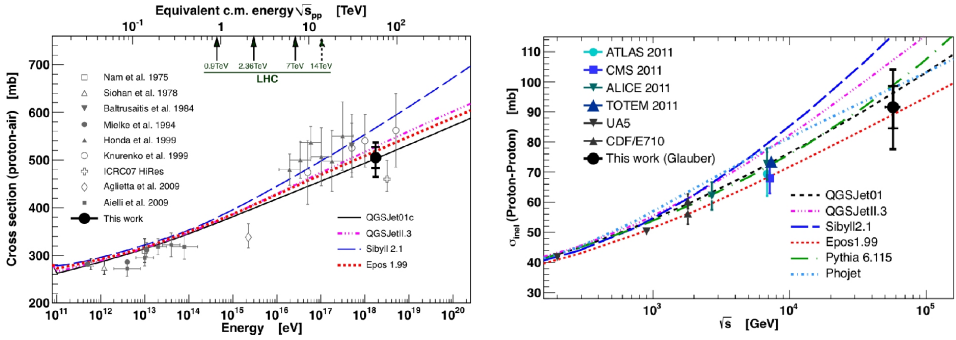

Fig. 4. $\sigma_{p-\mathrm{air}}$ as measured by the Pierre Auger Observatory (left). Conversion into σ_{p-p} applying the Glauber formalism (right) [10].

It is possible to use the Glauber model to translate this measurement into proton–proton cross section

$$\sigma_{p-p}^{\mathrm{Glauber}} = \left[92 \pm 7(\mathrm{stat})^{+9}_{-11}(\mathrm{sys}) \pm 11(\mathrm{Glauber})\right] \ \mathrm{mb}\,. \tag{3}$$

Our result [10] favours a moderately slow rise of the cross section with energy, in accordance with recent results from the LHC (*e.g.* [11]).

4.2. Number of muons at ground level

For inclined events, the electromagnetic signal is mostly absorbed by the atmosphere, and the signal registered by the SD is almost purely muonic. Therefore, the footprint of these events is proportional to the total number of muons of the shower. This is characterised by N_{19}, which represents the ratio to a benchmark model.

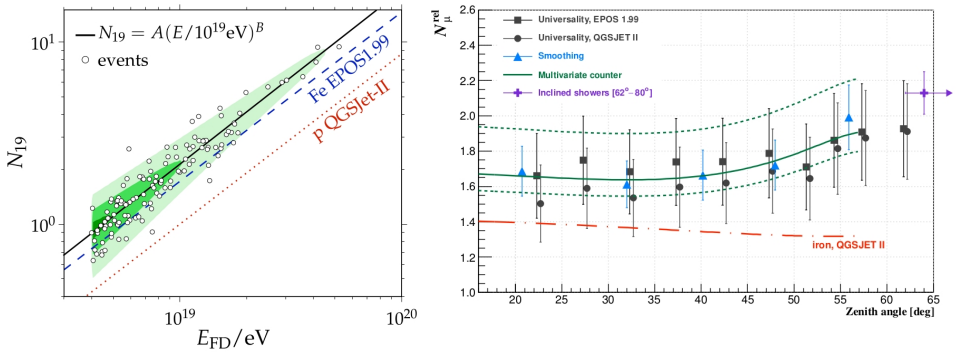

Fig. 5. Muon excess observed via N_{19} for inclined events (left). Confirmation by other techniques and zenith dependence (right) [5, 12].

Figure 5 shows how current models have difficulties to accommodate the Auger data, even in the muon-richest scenario [5]. This result is interpreted as a *muon excess* in real data as compared to simulations, and its origin is unclear. Several techniques have been developed to measure the muonic content of showers [12], with the similar outcome (Fig. 5). The muon deficit shows a dependence with zenith angle. Our data can be used to constrain hadronic interaction models at the highest energies ever probed.

5. Conclusions

The Pierre Auger Observatory is the largest cosmic ray experiment ever built, and it has been accumulating a massive set of data for almost a decade now. It has measured the end of the cosmic ray energy spectrum with unprecedented statistics, confirming the existence of the ankle and a large suppression at the highest energies.

The mass composition analyses clearly disfavour a pure-proton composition, and indicate a trend towards heavier composition as the energy grows. However, the interpretation of these results relies heavily on high energy hadronic interaction models, which show some stress with current data, especially in the number of muons at ground.

The Pierre Auger Observatory provides a measurement of the proton–proton cross section at the highest energy achieved so far, through the measurement of proton–air cross section and the Glauber formalism.

I would like to thank A. Bueno for carefully revising the manuscript. This work has been funded by the Ministerio de Economía y Competitividad.

REFERENCES

[1] J. Abraham *et al.*, *Nucl. Instrum. Methods* **A523**, 50 (2004).
[2] V. Berezinksy, A.Z. Gazizov, S.I. Grigorieva, *Phys. Rev.* **D74**, 043005 (2006).
[3] R. Aloisio, V. Berezinksy, A.Z. Gazizov, *J. Phys. Conf. Ser.* **337**, 012042 (2012).
[4] P. Abreu *et al.*, *Astropart. Phys.* **34**, 368 (2011).
[5] P. Abreu *et al.*, `arXiv:1107.4809 [astro-ph]`.
[6] A. Aab *et al.*, `arXiv:1307.5059 [astro-ph]`.
[7] A. Letessier-Selvon *et al.*, `arXiv:1310.4620 [astro-ph]`.
[8] P. Abreu *et al.*, *JCAP* **1302**, 026 (2013).
[9] T.K. Gaisser, *Cosmic Rays and Particle Physics*, Cambridge Univ. Press., 1991.
[10] P. Abreu *et al.*, *Phys. Rev. Lett.* **109**, 062002 (2012).
[11] A.J. Zsigmond *et al.*, `arXiv:1205.3142 [hep-ex]`.
[12] A. Yushkov, *Eur. Phys. J. Web. Conf.* **53**, 07002 (2013).